

Atlas-Based Interpretable Age Prediction In Whole-Body MR Images

Sophie Starck^{*1}, Yadunandan Vivekanand Kini^{*1}, Jessica Johanna Maria Ritter², Rickmer Braren², Daniel Rückert^{1,2,3}, and Tamara Müller^{1,2}

¹ Chair for AI in Medicine and Healthcare, Faculty of Informatics, Technical University of Munich, Germany

² Department of Diagnostic and Interventional Radiology, Faculty of Medicine, Technical University of Munich, Germany

³ Department of Computing, Imperial College London, United Kingdom

Abstract. Age prediction is an important part of medical assessments and research. It can aid in detecting diseases as well as abnormal ageing by highlighting the discrepancy between chronological and biological age. To gain a comprehensive understanding of age-related changes observed in various body parts, we investigate them on a larger scale by using whole-body 3D images. We utilise the Grad-CAM interpretability method to determine the body areas most predictive of a person’s age. We expand our analysis beyond individual subjects by employing registration techniques to generate population-wide interpretability maps. Our findings reveal three primary areas of interest: the spine, the autotthonous back muscles, and the cardiac region, which exhibits the highest importance.

1 Introduction

Deep learning (DL) methods have significantly advanced medical research by delivering insights into normal physiology and disease processes. It can provide imaging-derived biomarkers for non-invasive predictions and support physicians in their work [43,31]. Given the high sensitivity of medical data and the potentially life-altering impact that can result from using DL models for medical diagnoses or interventions, incorporating interpretability methods is of great importance. Gaining a better understanding of these models, often referred to as “black boxes” that hide the details of the decision-making process, is highly relevant. It fosters trust, enhances usability, and could potentially even shed light on previously unknown correlations [2].

The investigation of ageing, age-related diseases, and the identification of specific areas in the body affected by age have been prominent research areas in medicine. Age shows one of the strongest correlations with the development

* These authors contributed equally.

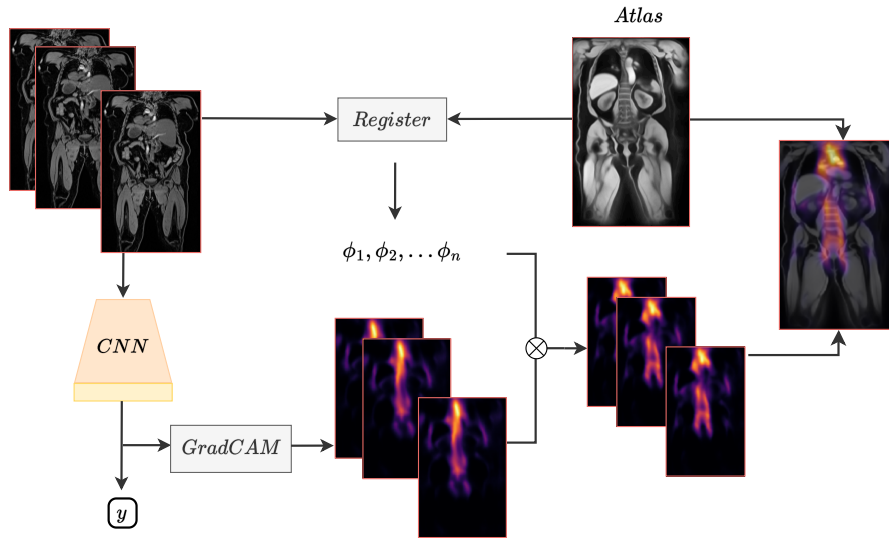


Fig. 1: Overview of the pipeline used in this work; First, the CNN is trained to predict age. From the trained model, at inference, Grad-CAM visual explanations are extracted for each subject and then mapped to an atlas before being averaged into a population-wide importance map.

of diseases and well-being in general [26,35]. Therefore, acquiring more knowledge about the ageing process can give insights into risk factors or abnormal ageing and serve as an early detection mechanism for several diseases [8]. The application of an accurate age prediction method is two-fold: (a) It can aid in establishing an understanding of the mechanisms of ageing in the human body and (b) in finding discrepancies between an individual’s chronological and biological age. Chronological age refers to the time elapsed since birth, whereas biological age aims to describe the physiological age, e.g. how the body has aged. There might be deviations between the two, which is often referred to as *accelerated* (biological age > chronological age) or *decelerated* (biological age < chronological age) ageing. This has been investigated extensively for brain age estimation [32] since brain structures are known to change over time [7,12] and be highly correlated with neurodegenerative diseases such as Alzheimer’s or Parkinson’s [20]. Brain MR images are promising modalities to infer the biological brain age of a subject, often with the help of deep learning techniques [32]. Age estimation has also been performed on dental data [42], skeleton bones in the body, such as chest radiography [25], knee skeletons [21], or hand skeletons [4]. Despite significant changes in several abdominal organs and tissues, such as the liver [40], bone densities [44], and the pancreas [24], whole-body age prediction has so far not been explored in great detail. There are however some works showing significant advancements in the field. Le Goallec et al. [19], for example, focus on deep

learning approaches for abdominal age prediction based on liver and pancreas MR images and Langner et al. [18] also investigate interpretable whole-body age prediction on 2D images.

Following the approach from Langner et al. [18], we investigate age prediction on the whole body (excluding the brain) to identify which areas show the highest information value about a person’s age, utilising the capacity of the whole 3D volumes. Towards this goal, we train a convolutional neural network (CNN) on 3D MR images that cover the full body from neck to knee. Subsequently, we apply Grad-CAM [36], a well-established post-hoc interpretability method for CNNs, to identify areas in the body that are most important to the algorithm’s decision-making. We subsequently register the Grad-CAM results onto a medical atlas to acquire population-wide interpretability maps. Figure 1 shows an overview of the pipeline of our work. We identify three main regions of interest in the extracted importance maps: the spine, the autochthonous back muscles, and the heart with its adjacent great vessels like the aorta. Figures 2 and 3 show two atlas-based importance maps. We can see that the region along the spine and the area surrounding the heart show the most prominent Grad-CAM activation.

2 Background and Related Work

In this section, we summarise relevant background and related works that address interpretability in medical imaging, age prediction and population-wide studies with medical atlases.

2.1 Interpretability

Interpretability methods are applied to DL algorithms to increase trust and reliability of DL models and better understand the decision-making process of neural networks [2]. This is especially important in the medical domain, where critical patient diagnoses might depend on DL predictions, and both physicians and patients need to trust the outcome of DL models to ensure their usability. One of the most commonly used interpretability method is gradient-weighted class activation mapping (Grad-CAM) [36]. Grad-CAM utilises the gradient information that flows into a convolutional layer of a CNN and applies global average pooling on these gradients to extract importance values for each input parameter (i.e. voxel). Grad-CAM was originally designed for image classification, image captioning, and virtual question-answering tasks [36]; it has, since then, been applied for numerous tasks such as object detection or reinforcement learning [16,6]. However, it has been shown that it can also produce meaningful interpretations for regression tasks [3].

One shortcoming of gradient-based interpretability methods such as Grad-CAM is that the results are subject-specific and do not allow for a population-wide interpretation. In the medical context, subject-specific interpretation can be of interest in individual assessments, while a population-level map might hold more generalisable information. We tackle this by generating population-wide interpretability maps using registration methods on previously unseen data.

2.2 Population-wide Studies and Medical Atlases

Medical imaging is indispensable for medical research and assessment. However, medical images mostly come with high inter-subject variability that can stem from different morphologies or even just different positions in the scanner. Therefore, medical atlases are frequently used to allow for inter-subject or inter-population comparisons. They map several medical images into a common coordinate system, using registration techniques [22]. The registered images are then averaged in order to acquire a template of a specific image modality. This is widely used for brain imaging, where atlases are used to generate an average representation of the human brain [15,23,41]. Atlas generation on the whole body has been explored considerably less due to a much higher inter-subject variability compared to brain images. However, there are some works focusing on body MR atlas generation that have shown promising applications for these atlases [37,39].

In this work, we utilise conditional atlases generated on a subset of the whole population, split by sex and BMI group (healthy, overweight, obese). Consequently, we obtain six comprehensive whole-body atlases. We utilise Grad-CAM to generate subject-specific importance maps which are subsequently aligned with these atlases, yielding population-wide importance maps.

2.3 Age prediction

Ageing is the main risk factor for disease development and it is an important indicator of a person’s overall health. MR images in particular hold great potential in the investigation of the physiological effects of ageing, and subsequently identifying diseases. For instance, Deep Learning methods have been extensively applied for brain age estimation, achieving a near-accurate age prediction with an error of 2.14 years. Age prediction has also been investigated on different body regions such as the teeth [42], the chest [25], knees [21], etc. Le Goallec et al. [19], have been focusing on abdominal age prediction from liver and pancreas MR images and achieve a mean absolute error (MAE) of 2.94 years. Langner et al. [18] perform interpretable age prediction on whole-body images and achieve a performance of 2.49 years with 2D projections of whole-body MR images from the UK Biobank. They aggregate the resulting saliency maps by co-registering the dataset onto a single representation.

In this work we extend the 2D approach from Langner et al. to 3D in order to better capture the contextual information inducing the ageing process. We subsequently register the data onto multiple curated atlases conditioned on physiological parameters, to be able to investigate subgroups effects of ageing.

3 Materials and Methods

3.1 Dataset

The UK Biobank (UKBB) dataset [30] is a large-scale longitudinal study that has been conducted in the UK since 2006. It contains information from approximately

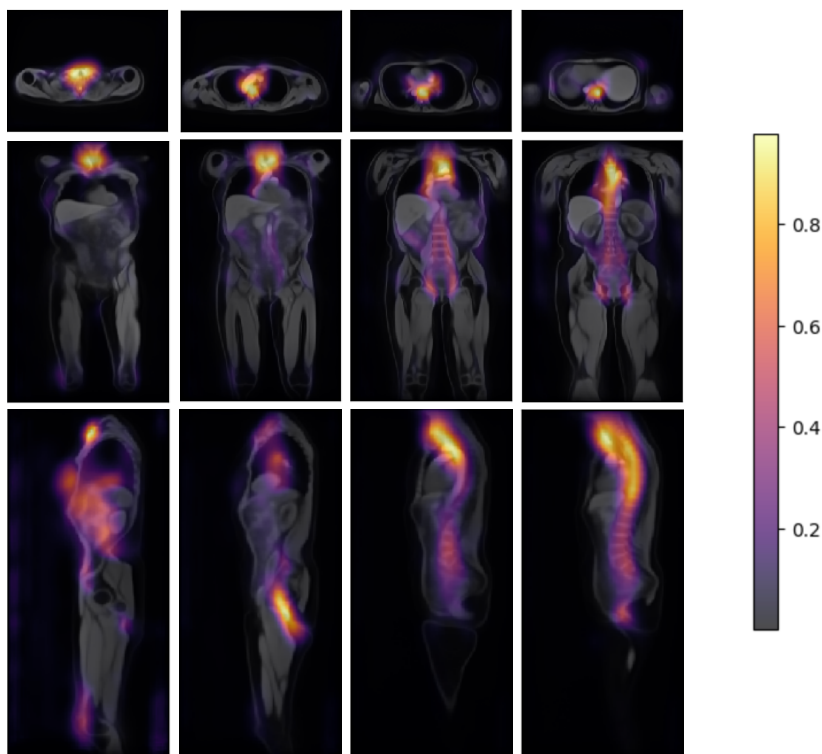


Fig. 2: Visualisation of the population-wide Grad-CAM activation maps across several slices overlaid on the healthy female atlas.

100,000 participants, with a wide range of data such as genetics, biological samples and MR images from the brain, heart and abdomen. In this work, we utilise the whole-body neck-to-knee MR images acquired with the Dixon technique for internal fat across six stations. We use the water contrast images and stitch the stations together using a publicly available tool [13]. We select 3120 subjects with a balanced distribution across age, sex and BMI. 1536 subjects were used for training, 384 for validation and 1200 for testing. The ages range from 46 to 81, and the mean age is 63.58 years.

3.2 Training Pipeline

We train a 3D ResNet-18 model [11,9] from torchvision [29] with a hidden layer size of 256. The training is performed by using adaptive moment estimation (Adam) optimiser [17] and by minimising the mean absolute error (MAE) of the age predictions. Furthermore, we use a gradient accumulation scheduler which sums and averages the gradients from 32 consecutive mini-batches to update the model’s parameters. The initial learning rate is $1e-4$, derived from manual

tuning and reduced via scheduling when the validation error does not decrease for three epochs. The model was trained for 100 epochs, which lasted approximately 48 hours on an NVIDIA A40 GPU.

The application of Grad-CAM is independent of the training process. After training the model, we apply Grad-CAM on the third layer of the network using the implementation from [10]. We apply Grad-CAM at inference and on the test set to evaluate the essential body areas related to age prediction.

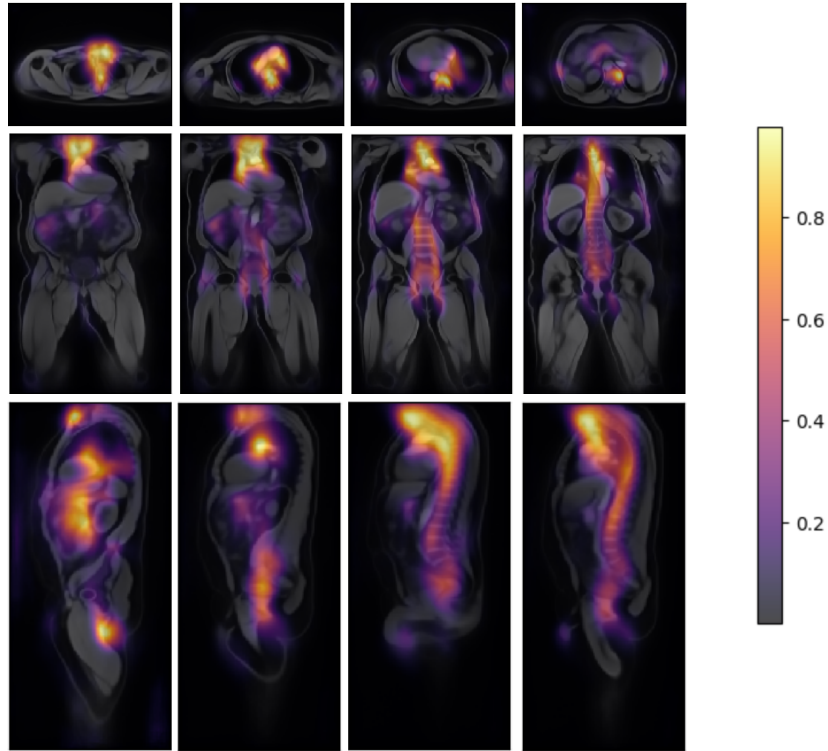


Fig. 3: Visualisation of the population-wide Grad-CAM activation maps across several slices overlaid on the obese male atlas.

3.3 Registration and Atlas Generation

We map all subject-level Grad-CAM maps onto an atlas to investigate the interpretability of our age prediction on a population level. Given the high variability of whole-body MR scans, we split all subjects into subgroups depending on their sex and BMI, following three commonly used BMI groups: healthy, overweight,

and obese following the pipeline proposed in [38]. We therefore use the six distinct atlases constructed by [38] available on a public platform. The registration process is done by first registering all images of a sex and BMI group to the same target subject. We apply two methods: affine and deformable registration. Affine registration refers to a set of rigid transformations such as rotation, translation, shearing and scaling. These types of transformations allow for a coarse alignment; they do not deform the anatomy of the given subject but only correct the overall position and orientation. The resulting images are then deformed with a non-rigid registration for a more refined registration. This step is more localised and allows for a more detailed alignment. Both registration steps were performed using the publicly available registration tools MIRTk [33] and deepali [34], all parameters are reproduced from [38]. Once all images are registered, the resulting deformation fields are applied to their corresponding activation map, as shown in Figure 1. Subsequently, an average map is generated from each subgroup of the dataset which serves as our population-wide interpretability map.

4 Results and Discussion

We here summarise the results obtained from our experiments, including the age prediction, the extraction of the Grad-CAM importance maps, and the generation of a population-wide importance map, and discuss our findings.

Table 1: Summary of the age prediction results by sex and BMI group on the test set. All values are reported MAE scores in years. The *Overall* column and row report the MAE of both sexes or all BMI groups, respectively. The score on the whole test set is underlined.

	Healthy	Overweight	Obese	Overall
Female	2.766	2.730	2.819	2.772
Male	2.603	2.812	2.830	2.748
Overall	2.684	2.771	2.825	<u>2.760</u>
Mean prediction	7.439	7.748	7.298	7.499

4.1 Age Prediction and Grad-CAM results

We evaluate our 3D age prediction model, trained on 1536 training samples, by randomly extracting 1200 previously unseen subjects that are approximately equally distributed across all BMI and age groups. Our model achieves a mean absolute error (MAE) of **2.76** years on this test set. Table 1 summarises the model’s performance divided into the same groups that are used for the atlas generation, as well as the performance for mean prediction for each group. We

can see that the model performs much better than the mean prediction, which indicates that it is learning meaningful information. Furthermore, we can see that the model performs best on healthy subjects and performance decreases for the other BMI groups. Our model reaches comparable performance to existing age estimation methods such as the brain (2.14 years) and, abdomen (2.94 years) [19] or whole body (2.49 years) [18].

To extract the Grad-CAM importance maps, we follow the original approach introduced by [36]. We extract the importance maps from the inference runs of the 1200 test subjects (200 of each group) and register them to the sub-group atlases to obtain the population-wide attention maps shown in Figures 2 and 3. By visual assessment of these individual maps, we identify three main areas of importance: (1) the spine, (2) the autochthonous muscles of the back, and (3) the heart region, including the myocardium (muscle tissue surrounding the heart) and the great adjacent vessels (e.g. the aorta). These regions are consistently highlighted over every atlas. Additional highlighted regions comprise the thyroid gland, as we can see in the top left visualisation of both Figures 2 and 3, the knees (bottom left in Figure 2) and the abdominal fatty tissue (middle right in Figure 3). The additional regions show lesser importance but are identifiable in several groups. These findings align with related work from Langner et al. [18] as the same regions are consistently highlighted. The use of a 3D model allows for leveraging the entire volume and therefore discovering another major region of interest: the spine. Additionally, these findings concur with medical research, as these regions have demonstrated age-related impacts [14,28,27], which makes us believe that these population-wide activation maps have great potential to investigate those areas in the body that show the greatest changes with ageing.

5 Conclusion and Future Work

In this work, we investigate the locality of age information in whole-body MR images. We extend the work of Langner et al. [18] by training a 3D ResNet-18 model on around 1500 neck-to-knee MR images from the UK Biobank [30]. Our model achieves whole-body age prediction with a mean absolute error of **2.76** years on the test set. In order to investigate which parts of the body are highly predictive of a subject’s age, we apply Grad-CAM to the gradients derived from each test subject. The obtained individual importance maps for all subjects highlight three main regions of interest: the spine, the heart, and the autochthonous muscle. However, these importance maps are subject-specific and do not allow for an easy generalisation to the whole population. We tackle this by registering all importance maps into the same coordinate space and overlaying them with an extracted atlas of the whole-body MR images. The results of these population-wide importance maps are visualised in Figures 2 and 3. Despite mapping individual importance maps to the population atlas and across various groups, these areas stay consistent. Hence, we can deduce that these findings remain valid for the entire population.

Moreover, the most highlighted areas of the importance maps align with medical knowledge and previous works about ageing. This shows promise in investigating the resulting importance maps in more detail with medical experts to potentially unveil knowledge on ageing in previously unexplored body regions. Leveraging the whole 3D volume allows for qualitative and reliable interpretability maps but has the major drawback of being slow and energy hungry. Using 2D approaches such as Langner et al. [18] allows for a faster training and therefore the integration of more data, but less detailed importance maps, which is a trade-off one might consider when using such methods. Furthermore, we recognise the opportunity to extract even more qualitative interpretability maps. We aim to further investigate different interpretability methods, such as perturbation-based methods [45] or attention-based models, such as Vision Transformers [5]. Moreover, we intend to implement this process on comparable datasets like the German National Cohort [1] to validate the broader applicability of these findings.

The ultimate target of generating these age-based importance maps is to investigate the mechanisms of ageing at a global scale and understand its behaviours. We can use the model’s performance to identify subjects that show accelerated or decelerated ageing, to investigate potential anomalies in their physiology. We believe that taking the interpretability maps from a subject-level to a population-level, allows us to draw more general conclusions about age-related areas in the human body which can guide future research of ageing and age-related diseases.

Acknowledgements TM and SS were supported by the ERC (Deep4MI - 884622). This work has been conducted under the UK Biobank application 87802. SS has furthermore been supported by BMBF and the NextGenerationEU of the European Union.

References

1. Bamberg, F., Kauczor, H.U., Weckbach, S., Schlett, C.L., Forsting, M., Ladd, S.C., Greiser, K.H., Weber, M.A., Schulz-Menger, J., Niendorf, T., et al.: Whole-body mr imaging in the german national cohort: rationale, design, and technical background. *Radiology* **277**(1), 206–220 (2015)
2. Carvalho, D.V., Pereira, E.M., Cardoso, J.S.: Machine learning interpretability: A survey on methods and metrics. *Electronics* **8**(8), 832 (2019)
3. Chen, L., Chen, J., Hajimirsadeghi, H., Mori, G.: Adapting grad-cam for embedding networks. In: *Proceedings of the IEEE/CVF Winter Conference on Applications of Computer Vision*. pp. 2794–2803 (2020)
4. Darmawan, M., Yusuf, S.M., Kadir, M.A., Haron, H.: Age estimation based on bone length using 12 regression models of left hand x-ray images for asian children below 19 years old. *Legal Medicine* **17**(2), 71–78 (2015)
5. Dosovitskiy, A., Beyer, L., Kolesnikov, A., Weissenborn, D., Zhai, X., Unterthiner, T., Dehghani, M., Minderer, M., Heigold, G., Gelly, S., et al.: An image is worth 16x16 words: Transformers for image recognition at scale. *arXiv preprint arXiv:2010.11929* (2020)

6. Dubost, F., Adams, H., Yilmaz, P., Bortsova, G., van Tulder, G., Ikram, M.A., Niessen, W., Vernooij, M.W., de Bruijne, M.: Weakly supervised object detection with 2d and 3d regression neural networks. *Medical image analysis* **65**, 101767 (2020)
7. Esiri, M.M.: Ageing and the brain. *The Journal of Pathology: A Journal of the Pathological Society of Great Britain and Ireland* **211**(2), 181–187 (2007)
8. Fayosse, A., Nguyen, D.P., Dugravot, A., Dumurgier, J., Tabak, A.G., Kivimäki, M., Sabia, S., Singh-Manoux, A.: Risk prediction models for dementia: role of age and cardiometabolic risk factors. *BMC medicine* **18**, 1–10 (2020)
9. Feichtenhofer, C., Fan, H., Malik, J., He, K.: Slowfast networks for video recognition. In: *Proceedings of the IEEE/CVF international conference on computer vision*. pp. 6202–6211 (2019)
10. Gotkowski, K., Gonzalez, C., Bucher, A., Mukhopadhyay, A.: M3d-cam: A pytorch library to generate 3d data attention maps for medical deep learning (2020)
11. He, K., Zhang, X., Ren, S., Sun, J.: Deep residual learning for image recognition. In: *Proceedings of the IEEE conference on computer vision and pattern recognition*. pp. 770–778 (2016)
12. Huizinga, W., Poot, D.H., Vernooij, M.W., Roshchupkin, G.V., Bron, E.E., Ikram, M.A., Rueckert, D., Niessen, W.J., Klein, S., Initiative, A.D.N., et al.: A spatio-temporal reference model of the aging brain. *NeuroImage* **169**, 11–22 (2018)
13. I, L., B, G., D, R., SA, T., EO, A., AG, R.: Machine learning in whole-body mri: experiences and challenges from an applied study using multicentre data. *Clinical Radiology* (2019)
14. Ignasiak, D., Valenzuela, W., Reyes, M., Ferguson, S.J.: The effect of muscle ageing and sarcopenia on spinal segmental loads. *European Spine Journal* **27**, 2650–2659 (2018)
15. Insel, T.R., Landis, S.C., Collins, F.S.: The nih brain initiative. *Science* **340**(6133), 687–688 (2013)
16. Joo, H.T., Kim, K.J.: Visualization of deep reinforcement learning using grad-cam: how ai plays atari games? In: *2019 IEEE Conference on Games (CoG)*. pp. 1–2. IEEE (2019)
17. Kingma, D.P., Ba, J.: Adam: A method for stochastic optimization. *CoRR* **abs/1412.6980** (2014)
18. Langner, T., Wikström, J., Bjerner, T., Ahlström, H., Kullberg, J.: Identifying morphological indicators of aging with neural networks on large-scale whole-body mri. *IEEE transactions on medical imaging* **39**(5), 1430–1437 (2019)
19. Le Goallec, A., Diai, S., Collin, S., Prost, J.B., Vincent, T., Patel, C.J.: Using deep learning to predict abdominal age from liver and pancreas magnetic resonance images. *Nature Communications* **13**(1), 1979 (2022)
20. Luders, E., Cherbuin, N., Gaser, C.: Estimating brain age using high-resolution pattern recognition: Younger brains in long-term meditation practitioners. *Neuroimage* **134**, 508–513 (2016)
21. Maggio, A.: The skeletal age estimation potential of the knee: Current scholarship and future directions for research. *Journal of Forensic Radiology and Imaging* **9**, 13–15 (2017)
22. Maintz, J.A., Viergever, M.A.: A survey of medical image registration. *Medical image analysis* **2**(1), 1–36 (1998)
23. Markram, H.: The human brain project. *Scientific American* **306**(6), 50–55 (2012)
24. Meier, J.M., Alavi, A., Iruvuri, S., Alzeair, S., Parker, R., Houseni, M., Hernandez-Pampaloni, M., Mong, A., Torigian, D.A.: Assessment of age-related changes in

- abdominal organ structure and function with computed tomography and positron emission tomography. In: *Seminars in nuclear medicine*. vol. 37, pp. 154–172. Elsevier (2007)
25. Monum, T., Mekjaidee, K., Pattamapaspong, N., Prasitwattanaseree, S.: Age estimation by chest plate radiographs in a thai male population. *Science & Justice* **57**(3), 169–173 (2017)
 26. Niccoli, T., Partridge, L.: Ageing as a risk factor for disease. *Current biology* **22**(17), R741–R752 (2012)
 27. Oei, M.W., Evens, A.L., Bhatt, A.A., Garner, H.W.: Imaging of the aging spine. *Radiologic Clinics* **60**(4), 629–640 (2022)
 28. Paneni, F., Diaz Cañestro, C., Libby, P., Lüscher, T.F., Camici, G.G.: The aging cardiovascular system: understanding it at the cellular and clinical levels. *Journal of the American College of Cardiology* **69**(15), 1952–1967 (2017)
 29. Paszke, A., Gross, S., Massa, F., Lerer, A., Bradbury, J., Chanan, G., Killeen, T., Lin, Z., Gimelshein, N., Antiga, L., Desmaison, A., Kopf, A., Yang, E., DeVito, Z., Raison, M., Tejani, A., Chilamkurthy, S., Steiner, B., Fang, L., Bai, J., Chintala, S.: Pytorch: An imperative style, high-performance deep learning library. In: *Advances in Neural Information Processing Systems* 32, pp. 8024–8035. Curran Associates, Inc. (2019)
 30. Petersen, S.E., Matthews, P.M., Bamberg, F., Bluemke, D.A., Francis, J.M., Friedrich, M.G., Leeson, P., Nagel, E., Plein, S., Rademakers, F.E., et al.: Imaging in population science: cardiovascular magnetic resonance in 100,000 participants of uk biobank-rationale, challenges and approaches. *Journal of Cardiovascular Magnetic Resonance* **15**(1), 1–10 (2013)
 31. Piccialli, F., Di Somma, V., Giampaolo, F., Cuomo, S., Fortino, G.: A survey on deep learning in medicine: Why, how and when? *Information Fusion* **66**, 111–137 (2021)
 32. Sajedi, H., Pardakhti, N.: Age prediction based on brain mri image: a survey. *Journal of medical systems* **43**, 1–30 (2019)
 33. Schnabel, J.A., Rueckert, D., Quist, M., Blackall, J.M., Castellano-Smith, A.D., Hartkens, T., Penney, G.P., Hall, W.A., Liu, H., Truwit, C.L., Gerritsen, F.A., Hill, D.L.G., Hawkes, D.J.: A generic framework for non-rigid registration based on non-uniform multi-level free-form deformations. In: Niessen, W.J., Viergever, M.A. (eds.) *Medical Image Computing and Computer-Assisted Intervention – MICCAI 2001*. pp. 573–581. Springer Berlin Heidelberg, Berlin, Heidelberg (2001)
 34. Schuh, A., Qiu, H., HeartFlow Research: deepali: Image, point set, and surface registration in PyTorch. <https://doi.org/10.5281/zenodo.8170161>, <https://github.com/BioMedIA/deepali>
 35. Seale, K., Horvath, S., Teschendorff, A., Eynon, N., Voisin, S.: Making sense of the ageing methylome. *Nature Reviews Genetics* **23**(10), 585–605 (2022)
 36. Selvaraju, R.R., Cogswell, M., Das, A., Vedantam, R., Parikh, D., Batra, D.: Grad-cam: Visual explanations from deep networks via gradient-based localization. In: *Proceedings of the IEEE international conference on computer vision*. pp. 618–626 (2017)
 37. Sjöholm, T., Ekström, S., Strand, R., Ahlström, H., Lind, L., Malmberg, F., Kullberg, J.: A whole-body fdg pet/mr atlas for multiparametric voxel-based analysis. *Scientific Reports* **9** (2019)
 38. Starck, S., Sideri-Lampretsa, V., Ritter, J.J.M., Zimmer, V.A., Braren, R., Mueller, T.T., Rueckert, D.: Constructing population-specific atlases from whole body mri: Application to the ukbb (2023)

39. Strand, R., Malmberg, F., Johansson, L., Lind, L., Sundbom, M., Ahlström, H., Kullberg, J.: A concept for holistic whole body mri data analysis, imiomics. *PLoS one* **12**(2), e0169966 (2017)
40. Tajiri, K., Shimizu, Y.: Liver physiology and liver diseases in the elderly. *World journal of gastroenterology: WJG* **19**(46), 8459 (2013)
41. Van Essen, D.C., Smith, S.M., Barch, D.M., Behrens, T.E., Yacoub, E., Ugurbil, K., Consortium, W.M.H., et al.: The wu-minn human connectome project: an overview. *Neuroimage* **80**, 62–79 (2013)
42. Verma, M., Verma, N., Sharma, R., Sharma, A.: Dental age estimation methods in adult dentitions: An overview. *Journal of forensic dental sciences* **11**(2), 57 (2019)
43. Wang, F., Casalino, L.P., Khullar, D.: Deep learning in medicine—promise, progress, and challenges. *JAMA internal medicine* **179**(3), 293–294 (2019)
44. Wishart, J., Need, A., Horowitz, M., Morris, H., Nordin, B.: Effect of age on bone density and bone turnover in men. *Clinical endocrinology* **42**(2), 141–146 (1995)
45. Zeiler, M.D., Fergus, R.: Visualizing and understanding convolutional networks. In: *Computer Vision—ECCV 2014: 13th European Conference, Zurich, Switzerland, September 6–12, 2014, Proceedings, Part I* 13. pp. 818–833. Springer (2014)